Check for updates

Structured light

Andrew Forbes [1] ✉, Michael de Oliveira [1] and Mark R. Dennis [2]

All light has structure, but only recently has it been possible to control it in all its degrees of freedom and dimensions, fuelling fundamental advances and applications alike. Here we review the recent advances in 'pushing the limits' with structured light, from traditional two-dimensional transverse fields towards four-dimensional spatiotemporal structured light and multidimensional quantum states, beyond orbital angular momentum towards control of all degrees of freedom, and beyond a linear toolkit to include nonlinear interactions, particularly for high-harmonic structured light. Using a simple interference argument, centuries old, we weave a story that highlights the common nature of seemingly diverse structures, presenting a modern viewpoint on the classes of structured light, and outline the possible future trends and open challenges.

In a typical visible laser beam, there are potentially many millions of transverse modes per square millimetre[1], an extraordinary resource if it could be exploited. Yet for many years, only Gaussian beams were desired and the challenge was usually to remove unwanted transverse structure. This includes the many modes excited when looking through complex media, and in large aperture laser systems. In the early 2000s, tools such as liquid-crystal spatial light modulators[2], digital micromirror devices[3,4] and later geometric phase elements such as q-plates[5] and other spin–orbit approaches[6–8] matured to the extent that most laboratories could now reshape their light for some desired application, or even create it directly at the source[9]. An important example, of fundamental and practical interest, has been light beams structured to carry orbital angular momentum (OAM) (see refs. [10,11] and references therein). The result has been an explosion of activity in what is now referred to as structured light.

Perhaps the earliest account of structured light was by Thomas Young 200 years earlier (in 1803), when he demonstrated one-dimensional (1D) intensity structured light, that is, fringes, by interference of a plane wave through a double slit (in fact, around a strip of cardboard)[12]. Young's observation of fringe structure demonstrated the wave nature of light, with important information encoded in both the density and direction of the fringes. Today, these patterns are the basis of interferometry, underlying technology from medical imaging to structural engineering and discoveries from the nature of photons to gravitational wave detection. If this can all be achieved with sinusoidal fringes, what more might be possible with an arbitrarily sculpted light pattern? Already 100 years ago, Robert Wood understood that even orthogonally polarized beams could interfere, resulting in fringes in polarization. Structuring, in principle, can be expanded to all the degrees of freedom (DoFs) of a light beam and extends to the structuring of waves in many other systems, from sound to quantum matter, giving shape to the millions of lost modes.

In this Review, we outline recent advances in structured light, explain the role of interference in this development and present a modern zoology of structured light beams. We emphasize recent developments and breakthroughs in 'pushing the limits' beyond OAM, beyond 2D fields, beyond qubits and biphotons, and beyond linear optical manipulation, highlighting the open challenges that remain. While structured light has fuelled many applications, from imaging, microscopy, metrology, communication, quantum

information processing to light–matter interactions, we will not discuss them in any detail here (the reader is referred to refs. [13,14] and references therein); instead, we concentrate on the nature of structured light itself.

A zoology of structured light

We can discern many important principles when comparing an apparently unstructured plane wave with sinusoidal fringes. Most obviously, we can see the fringes as structuring the light's intensity, visible to the naked eye. A plane wave has structure too, in its uniform phase gradient, but this can only be seen with interferometry. Nevertheless, the direction of the phase change indicates the direction of energy flux via the Poynting vector. This flux, being the momentum carried by the light wave, provides the basis for optical trapping; although the phase flux is invisible, it can be felt.

While theoretically convenient, plane waves are not physically realizable in real optical systems, and the default 'light beam' we typically imagine in a laboratory has a transverse Gaussian profile. Its properties inform our expectations of the behaviour of light beams: its width expands upon propagation, while maintaining its intensity pattern, the Gouy phase endows it with a longitudinal phase dependence, and wavefront curvature leads to a transverse radial phase dependence. These properties follow from the fact that such a Gaussian beam is a mode of a resonant laser cavity, as are various other higher-order modes[15]. These higher cavity modes, known as transverse electromagnetic (TEM) modes, can take the form of Hermite–Gaussian (HG) beams, represented by a Gaussian profile times Hermite polynomials of order m in x and order n in y, with a slightly modified Gouy phase. Arising from astigmatism in the cavity, these carry an xy-grid structure from the zeros of the Hermite polynomials, which again expands with the beam. These naturally can be interpreted as the analogues of interference fringes carried by a Gaussian beam. Their Gouy phase depends on the mode order $N = m + n + 1$.

Going back to the early days of lasers[15], another family of beams was known, arising from a spherical aberration of the cavity mirrors: Laguerre–Gaussian (LG) beams. These are represented in cylindrical coordinates (r, ϕ, z) by an azimuthal oscillation of $\cos\ell\phi$ or $\sin\ell\phi$ times an associated Laguerre polynomial of order p, with $N = \ell + 2p + 1$ for positive integers ℓ and p. In 1992, Han Woerdman's group in Leiden, working with Les Allen, realized that complex LG beams are also possible, where the

Box 1 | Geometric representation

Just as for polarized light, a Poincaré sphere can be used to parameterize structured Gaussian modes[18]. LG modes, carrying oppositely signed OAM, sit at the north and south poles, like circular polarization states for the usual Poincaré sphere. HG modes with different orientations, like linear polarization, lie on the equator. The analogues of elliptic polarization states are the generalized Hermite–Laguerre–Gaussian beams (GHLG beam), which sit between LG and HG beams[127]. This allows many analogies to be drawn between optical polarization and structured Gaussian beams such as Pancharatnam–Berry phases. It can be used as a Bloch sphere analogue for structured beams as qubits for quantum information applications, where a unique sphere can be defined for each ℓ. The systems of LG, HG and GHLG beams can be transformed into each other by appropriate quantum-mechanical rotation transformations, and is a concrete physical realization of Schwinger's oscillator model of quantum angular momentum[128]. The Poincaré sphere combines both the amplitude and phase descriptions of the eigenstates into one visual description, defined by
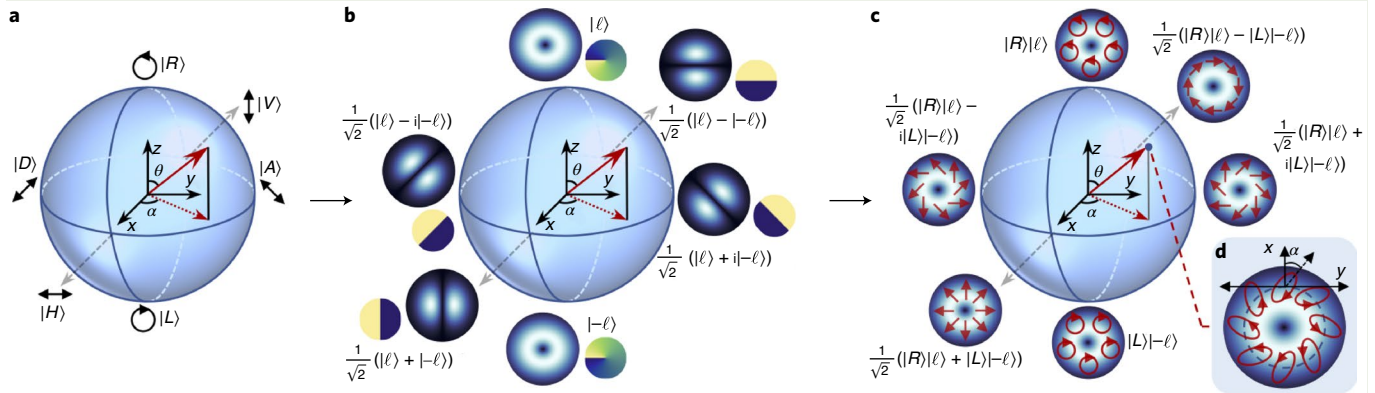
$$|\psi\rangle = \cos\left(\frac{1}{2}\theta\right)|R\rangle + e^{i\alpha}\sin\left(\frac{1}{2}\theta\right)|L\rangle,$$
$$\underbrace{\phantom{|\psi\rangle = \cos\left(\frac{1}{2}\theta\right)|R\rangle + e^{i\alpha}\sin\left(\frac{1}{2}\theta\right)|L\rangle}}_{\text{Polarization}}$$

$$|\psi\rangle = \cos\left(\frac{1}{2}\theta\right)|\ell\rangle + e^{i\alpha}\sin\left(\frac{1}{2}\theta\right)|-\ell\rangle,$$
$$\underbrace{\phantom{|\psi\rangle = \cos\left(\frac{1}{2}\theta\right)|\ell\rangle + e^{i\alpha}\sin\left(\frac{1}{2}\theta\right)|-\ell\rangle}}_{\text{OAM}}$$

$$(1)$$

with α describing the relative phase between states and θ describing the weighted contribution of each state. Furthermore, the Poincaré sphere representation has been extended to a higher-order Poincaré sphere[19,20], illustrating all the possible non-separable vector modes described by the tensor product of a particular combination of the polarization and OAM state spaces, given by

$$|\psi\rangle = \cos\left(\frac{1}{2}\theta\right)|\ell\rangle|R\rangle + e^{i\alpha}\sin\left(\frac{1}{2}\theta\right)|-\ell\rangle|L\rangle. \quad (2)$$
$$\underbrace{\phantom{|\psi\rangle = \cos\left(\frac{1}{2}\theta\right)|\ell\rangle|R\rangle + e^{i\alpha}\sin\left(\frac{1}{2}\theta\right)|-\ell\rangle|L\rangle}}_{\text{Polarization} \otimes \text{OAM}}$$

Analogously, the poles are scalar modes, whose superpositions form the maximally non-separable vector modes at the equator.

Geometric representation of paraxial structured light. a, Simultaneous control of the parameters α and θ, which correspond to the relative phase and weighted amplitude contributions, respectively, results in the description of a polarization state on a unit sphere expressed in terms of two orthogonal antipodal states. **b**, The Bloch sphere description for parametric structured light is analogous to the Poincaré sphere, with the poles corresponding to pure LG eigenstates. **c**, States on the surface of the higher-order Poincaré sphere are constructed from the tensor product of the polarization and OAM state spaces. **d**, Arbitrary spin–orbit coupled state showing the elliptical polarization orientation of the state, which is dependent on the parameter α. Here H, V, L, R, D and A represent the polarization states of horizontal, vertical, left, right, diagonal and antidiagonal, respectively.

real-valued cos or sin of $\ell\phi$ is replaced by an azimuthal phase increase of $\exp(\pm i\ell\phi)$. This is representative of a non-zero OAM carried by these beams[10]; this angular momentum around the beam centre is distinct from spin angular momentum (due to circular polarization), and led to 'optical spanners' manipulating the rotation of particles in optical traps[16]. Furthermore, such beams could be synthesized from HG beams in the lab with a cylindrical lens, analogous to the creation of circularly polarized light using linearly polarized light and a quarter-wave plate, or (more commonly these days) with computer-generated holograms[17]. The 'Poincaré sphere analogy' between HG and LG beams and
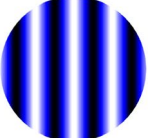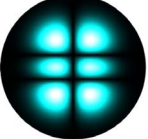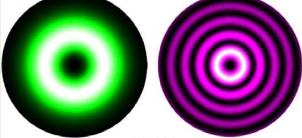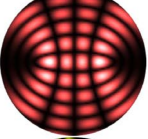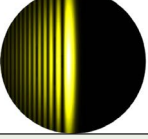
linearly and circularly polarized light has led to deeper insights in the area, providing a geometric representation (Box 1) of paraxial structured light[18–22].

As the complex structure of light beams appears to increase, it is desirable to understand the general principles behind them. One of surprising depth and generality has proved to be the study of optical singularities—special places in the beam where parameters such as phase are not defined[23,24]. For instance, along the axis of a complex LG beam carrying OAM, the phase is singular where the intensity is zero, with the equiphase surfaces—representing wavefronts—helically swirling around the axis. Although vortices and optical OAM

Box 2 | An operator representation

Operators for different kinds of 2D structured beams. Each beam family is a set of eigenfunctions for one or more given operators, where the eigenvalues may or may not have a simple physical interpretation. The overall beam behaviour is determined by a 'Hamiltonian' operator $\hat{\mathcal{H}}$. Gaussian beams are eigenfunctions of the beam quality factor operator $\widehat{\mathcal{M}}^2$, equivalent to the 2D quantum harmonic oscillator Hamiltonian. Propagation-invariant beams are eigenfunctions of the transverse Laplacian $-\nabla_\perp^2 = \hat{p}_r^2 = \hat{p}_x^2 + \hat{p}_y^2$, equivalent to the free 2D quantum Hamiltonian, and Airy beams to a Hamiltonian in a linear potential. In addition, OAM-carrying beams are eigenfunctions of angular momentum operator, $\hat{L}$, whereas the Cartesian-separated HG modes of the 'quality factor difference' operator $\widehat{M}$. The analogue $\widehat{M}$ for propagation-invariant beams is $\hat{p}_x^2 - \hat{p}_y^2$. Any superposition of the operators $\hat{L}$ and $\widehat{M}$ (with weightings α, β) has GHLG beams as eigenfunctions, all falling on the Poincaré sphere representation. IG and Mathieu beams are eigenfunctions of a superposition involving $\hat{L}^2$, allowing separation in elliptic coordinates.

Beam family (eigenfunctions)	Beam profile	Operator	Eigenvalue (if relevant)
Gaussian beams (waist width w_0)		Beam quality factor $\widehat{\mathcal{M}}^2 = \frac{r^2}{w_0^2} + \frac{k^2 w_0^2}{4}\hat{p}^2$	Mode order $N+1$
Propagation-invariant beams		Transverse Laplacian (free-space Hamiltonian) $\hat{p}^2$	k_r^2
HG beams HG_{mn}		Quality factor difference $\widehat{M} = \frac{x^2-y^2}{w_0^2} + \frac{k^2 w_0^2}{4}(\hat{p}_x^2 - \hat{p}_y^2)$	$m-n$
$\left\{\begin{array}{c} \text{LG beams } \mathrm{LG}_{\pm\ell p} \\ \text{Bessel beams } J_\ell(k_r r)\mathrm{e}^{i\ell\phi} \\ \text{(propagation invariant)} \end{array}\right\}$		Angular momentum $\hat{L} = x\hat{p}_y - y\hat{p}_x$	Angular momentum label $\pm\ell$
GHLG beams (label with m,n or $\pm\ell, p$)		Operator superposition $\alpha\hat{L} + \beta\widehat{M}$	Same eigenvalue $m-n = \pm\ell$
IG beam		Operator superposition $\alpha\hat{L}^2 + \beta\widehat{M}$	–
Mathieu beam (propagation invariant analogue of IG)		Operator superposition $\alpha\hat{L}^2 + \beta(\hat{p}_x^2 - \hat{p}_y^2)$	–
Airy beam		Quantum Hamiltonian with linear potential $\hat{p}^2 + \alpha x$	–

are not always found together, the vortex points in 2D, or filaments in 3D, provide a skeleton[23] on which the rest of the beam's amplitude is based. These singularities become particularly useful in light with a varying polarization state too, where spin–orbit effects[6,7] become important and the Poynting vector itself separates into separate spin and orbital contributions.

From the point of view of superpositions, each of the HG and LG modes form a complete basis that can represent any propagating
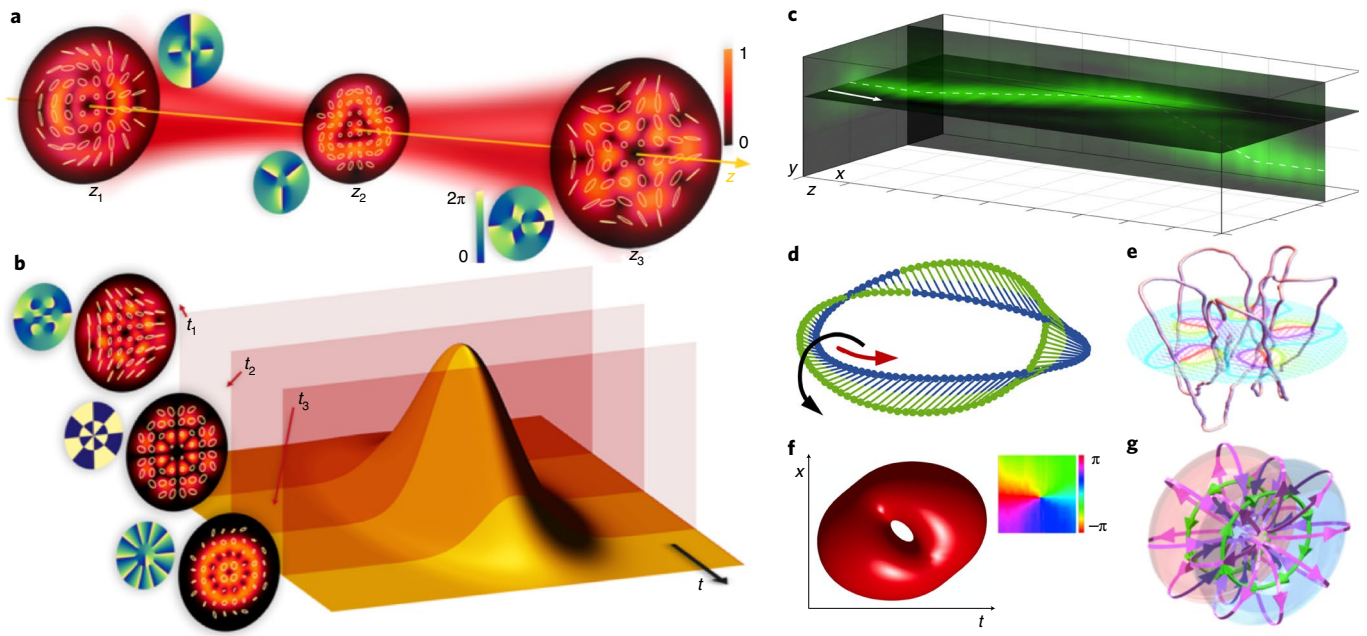
Fig. 1 | Beyond 2D structured light. To create 3D and 4D structured light requires control in many dimensions and DoFs. **a**, Full spatial control where each *z*-slice has a desired 2D profile for 3D structured light. **b**, Extending control to the time domain allows for 4D structured light, where analogously each time slice has a desired spatial profile. **c–f**, Examples of this 3D and 4D control include arbitrary trajectories of scalar light in space (**c**), Möbius polarization ribbons (**d**), polarization knots in space (**e**) and isosurface of a spatiotemporal optical vortex with measured phase in the *x–t* plane (**f**). **g**, The flying doughnut, a single-cycle toroidal pulse with electric (green) and magnetic (purple) field lines shown. Panels adapted with permission from: **c**, ref. [51], OSA; **d**, ref. [64], AAAS; **e**, ref. [65], Springer Nature Ltd; **f**, ref. [75], Springer Nature Ltd.

scalar beam. Using infinite sets of structured modes to represent light beams goes back at least to Stratton's classic textbook of the 1940s[25], where he chose an infinite set of Bessel modes to represent a cylindrical light beam. Like LG beams, Bessel modes have a $\cos\ell\phi$, $\sin\ell\phi$ or $\exp(\pm i\ell\phi)$ azimuthal dependence, but now multiplied by a radial Bessel function $J_\ell(k_r r)$ dependence[26] with a radial wavenumber, k_r. Unlike a Gaussian beam, they neither spread nor acquire a Gouy phase (in the idealized case): they are propagation invariant.

In all of the examples discussed so far, HG and LG beams, plane waves and Bessel beams, the structured beam can be represented in the 2D transverse plane as a product of functions in Cartesian (x, y) or polar (r, ϕ) coordinates. Although much less familiar, another natural 2D coordinate system is elliptical coordinates, given by systems of confocal ellipses and hyperbolas, and their propagation-invariant realizations are called Mathieu beams (as they are represented by Mathieu functions in the elliptic coordinates)[27]. Their Gaussian counterparts are Ince–Gaussian (IG) beams[28], with Ince polynomials playing the role of the Hermite and Laguerre polynomials previously. In fact, these also occur as cavity modes, naturally interpolating between HG modes and (real valued) LG modes. Propagation-invariant beams also allow separation in parabolic coordinates, for the realization of parabolic beams[29]. These classes can be grouped together as Helmholtz–Gauss beams[30] and written compactly as the product of a Gaussian beam times a *z*-dependent complex amplitude and a function that depends on the coordinate system of interest: plane waves in Cartesian coordinates, Bessel beams in cylindrical coordinates, Mathieu beams in elliptical coordinates and parabolic beams in parabolic cylindrical coordinates.

How can we approach such a confusing menagerie of different possibilities? One natural approach is inspired by the fact that classical light is subject to the principles of wave mechanics: the paraxial equation $-\nabla_\perp^2 \psi = ik\partial_t \psi$ (where all terms have their usual

meaning) resembles the free 2D time-dependent Schrödinger equation, and for propagation-invariant beams, the transverse Helmholtz equation $-\nabla_\perp^2 \psi = k_r^2 \psi$ resembles the free 2D time-independent Schrödinger equation. Thus, our structured light beams can be considered as analogous to structured 2D quantum wavepackets, whose time evolution is equivalent to propagation in *z*. Inspired by this approach, we can identify operators for which our beam families are eigenfunctions[31,32].

An obvious example is the angular momentum operator $\hat{L} \equiv -i\partial_\phi$, with eigenvalues $\pm\ell$ and OAM eigenfunctions $\propto e^{\pm i\ell\phi}$, giving complex LG or Bessel beams. The real-valued cases, insensitive to the sign of phase winding, are eigenfunctions of $\hat{L}^2$, which allows for eigenfunctions $\propto e^{i\ell\phi} + e^{-i\ell\phi} \propto \cos\ell\phi$. Even a plane wave, say $e^{ik_x x}$, is an eigenfunction of the transverse linear momentum operator $\hat{p}_x = -i\partial_x$ with eigenvalue k_x, and the interference pattern $\cos k_x x$ is equivalently an eigenfunction of $\hat{p}_x^2 = -\partial_x^2$. As Gaussian beams resemble eigenstates of the 2D quantum harmonic oscillator—with parabolic cavity mirrors acting like a quadratic potential—they are eigenfunctions of the $\mathcal{M}^2$ operator, which is analogous to a quantum harmonic oscillator Hamiltonian. In fact, all of the beams described above can be described as eigenfunctions of linear and angular momentum operators or combinations of them (Box 2).

Very far from the non-diffracting case, Airy beams—based on Airy functions originally defined to explain supernumerary interference fringes below a rainbow—appear to accelerate transversely upon propagation[33]. These were inspired from the stationary quantum-mechanical solution of a particle in a linear potential; if the potential is removed, they appear to accelerate under paraxial (that is, Schrödinger) evolution[34]. As for the rainbow, it is natural to approximate Airy functions semiclassically by using geometric optical rays carrying a phase, with the fringes being interpreted as interfering rays, and the bright regions as caustics. In fact, the

detailed structure of caustics (studied historically by Leonardo da Vinci, Hamilton, Stokes and others including Airy), occurring even in incoherent light, offers another route to structured light. Rays and caustics can be identified for the Gaussian and propagation-invariant families described above, as the families of classical trajectories associated with the quantum wavepacket interpretation of the light beams[32]. The quantum analogy even extends to the polarization of classical light beams if we associate two orthogonal polarization states (linear and horizontal, or right- and left-handed circular) with quantum spin up and spin down. Combining differently structured beams with orthogonal polarization states gives position-dependent polarization patterns. This non-separability of the spin and position-dependent DoFs of the classical optical field is sometimes interpreted as the classical analogue of quantum entanglement[35]. This not only gives new insight into these fundamental phenomena but also offers crucial improvements to optimizing modes for quantum communication systems, whose natural sets of modes do not have a simple factorization into amplitude and polarization.

Beyond two dimensions

Conventional structuring of optical fields is often restricted to the two dimensions of the transverse plane and left to propagate in the third dimension, z. We will call this 2D control. Less mature, but receiving intense interest, is the ability to tailor light beyond two dimensions, towards 3D control (in all spatial coordinates and field components) and finally (3 + 1)D structured light fields by spatio-temporal control, as illustrated in Fig. 1a,b, respectively.

Three-dimensional structured light. Three-dimensional control is immediate in systems that confine the light (for example, photonic crystals) where the marriage of structured matter and structured light has opened many exciting prospects[36]. Between this and free space is the possibility to tailor light by a cascade of custom phase elements[37–40], transforming one or many modes, and guiding them in space. This is a powerful approach to execute unitary operations on multimodal classical light[41] and high-dimensional quantum states[42]. A more common approach is to control light's structure in three dimensions by judiciously setting the DoFs of the initial 2D field, and by wave interference create the desired structure, for example, the Talbot effect and fractal light[43]. A popular example is the construction of Bessel beams, where the interference of many plane waves travelling on a cone ensures that the non-diffracting nature occurs over some distance. By forcing the plane waves in the initial 2D field to have a common radial wavevector (k_r), which is easily achieved with just an annular ring, they accumulate phase at the same rate as they propagate. At each z plane, the conical waves arrive with the same relative phase so the interference pattern (the 2D field) remains invariant during propagation. By exploiting the phase inside the ring as a free variable, any optical field can be made non-diffracting in three dimensions[44], while subwavelength-scaled versions are possible from simple sharp-edged diffraction by high-spatial-frequency wave interference[45].

Perhaps the simplest 3D control is to borrow tools from structured illumination and apply them to structured light. A topical example of this is light sheets, where the 'thin' 2D structured field is scanned (changing the initial wavevectors by a linear phase) so that its optical path selectively fills a large volume one slice at a time. This is a crucial tool in microscopy as it enables rapid, high-contrast volumetric imaging with little sample exposure[46]. In such light-sheet microscopy, structuring the field that is scanned has proven essential, for example, Bessel beams for increased field of view[47] and Airy beams for better contrast[48]. To improve further requires full control of the field along the propagation direction. One such approach is to return to the notion of interference as the cornerstone of structured light, but replacing the ubiquitous plane waves with 2D tai-
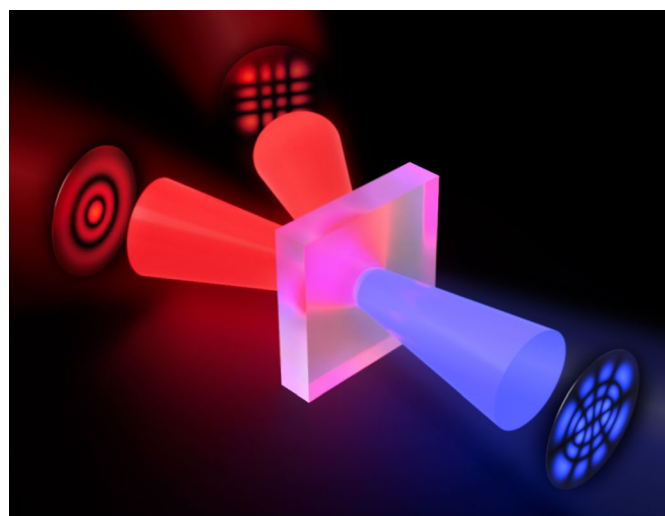

Fig. 2 | A nonlinear toolbox. There is a growing trend towards enhancing linear tools with nonlinear functionality. Mode converters, traditionally the realm of linear optics, are now possible by nonlinear wave mixing. In this artistic impression, HG and LG modes are combined to form a new IG mode. A slightly modified process allows for nonlinear structured light detectors, both of which have been demonstrated experimentally[85,86].

lored light. Summing many Bessel beams with carefully selected but differing radial wavevectors sets both the ring spacing (transversal control) and the z-dependent phases (propagation control) simultaneously, for 3D control of the field in some desired propagation interval[49]. Splicing the intervals together allows for exotic 3D behaviour, including z-dependent wavelength and topological charge control[50], light following arbitrary trajectories in space[51] (as shown in Fig. 1c), attenuation compensated propagation for looking deep into scattering media[52], discrete-like diffraction[53], quantum random walks in free space[54], as well as angular[55] and radial[56] accelerating light. In a similar manner, superpositions of Airy beams have been used to construct abruptly focusing light[57], which has proved useful in delivering high-intensity light at localized positions in space. Even summing simple plane waves can be exploited for exotic 3D response if their full DoFs are controlled, for example, for synthetic chiral light in 3D by the superposition of just two planes waves with differing polarizations, wavelengths and spatial frequencies (angles)[58].

Attracting much attention is the ability to tailor light in all three components of the fields, often by exploiting the wide angular spectrum available in non-paraxial light. By reverse propagating the desired field using the vector diffraction tools of Richards and Wolf, the required initial amplitude, phase and polarization structure can be deduced. Recently, simple recipes have emerged to structure the longitudinal component of the electric field (E_z) at a focus by judicious shaping an initial 2D field[59,60]. Control of the transverse fields ($E_\perp$) is simultaneously possible because the solution may be adjusted by a 2D solenoidal potential without altering the desired longitudinal field, giving a DoF to create 3D structured light. Such 2D polarization structuring of the initial field opens unprecedented control for exotic 3D structures[61], including 3D polarization standing waves[62,63], polarization Möbius strips[64] and knotted polarization structures in space[65], with examples shown in Fig. 1d,e.

This 3D control has given rise to a new research direction: tailoring angular momentum states from longitudinal to transverse, such as photonic wheels[66] by tight focusing of opposite spin states or by simple two-wave interference[67]. Interestingly, the transverse spin component in non-paraxial light is independent of the

initial polarization state, existing even for unpolarized light. This is because the 2D state of unpolarized light has one random phase between the two orthogonal components, whereas, in three dimensions, completely unpolarized light requires two random phases between the three field components. The implication is that if 3D polarization structured light is created from an initial 2D structure through some optical transformation (which does not introduce any randomness), then there will always be some degree of polarization (P) in the 3D field of $\frac{1}{2} \leq P \leq 1$ due to spin–orbit coupling[68], and can be tailored to be fully 3D polarized even from an initially paraxial unpolarized 2D structure[69].

Four-dimensional structured light. Adding temporal control to the 3D spatial control allows for the creation of $(3+1)$D structured light, or what we will call 4D structured light. Placing a beam-shaping device between two gratings in a $4f$ system allows the spectral components to be modulated in amplitude and phase, which then recombine for temporal control[70]. A second device for spatial control gives the possibility of setting the initial parameters in both domains, with some modern possibilities to simultaneously tailor based on both liquid-crystal topological structures[71] and active metasurfaces[72,73]. Such approaches have been used to produce spatiotemporal Bessel beams[74], and more recently, spatiotemporal vortices as 'optical cyclones'[75], where the wave packet has a spiral phase in the meridional x–t plane for a transverse OAM, shown in Fig. 1f. In the context of interference, it is the superposition of many frequency components with appropriate amplitude and phase that makes this control possible.

A quick inspection of the propagation equations in space and time reveal two interesting features: first, spatial diffraction in free space is analogous to temporal dispersion in media with a wavelength-dependent refractive index, but while the former is always positive, leading to spatial spreading, the latter can lead to a widening, narrowing or no effect at all on the temporal pulse; second, the spatial and temporal DoFs couple under even the simplest transformations[76,77]. This has been exploited to control 3D arrays of spatiotemporal foci, for simultaneous focusing in space and time, using just a microscope objective and a spatial light modulator[78]. Key to these types of approach is space–time coupling: when an ultrafast laser pulse is passed through an objective lens, in the pupil plane there is a space-to-frequency mapping of $r(\omega) \propto \omega$, so that changing the spectral properties of the pulse also changes its spatial properties, and vice versa. Such techniques are driving high-precision multiplane imaging and materials processing, often combined with penetrating deep into complex media through 4D structured light[79]. This coupling can also be exploited to create spatially non-diffracting beams through temporal control, where diffraction is compensated by dispersion[80]. The idea is best viewed from the perspective of a 1D beam, where $k_z^2 = (\omega/c)^2 - k_x^2$ (c is the speed of light in vacuum) so that each transverse wavevector (k_x) is associated with a multitude of frequencies, ω, and thus many axial wavenumbers (k_z): diffraction compounded by dispersion. By selecting an isosurface in (k_x, ω) space where $(\omega/c)^2 - k_x^2 =$ constant, all plane waves will have the same k_z, even though each transverse wavevector is associated with a unique frequency. As all the plane waves add with the same phase, the result is a non-diffracting beam, engineered by space–time coupling, and can be extended to creating arbitrary non-diffracting 1D space–time light sheets[81], in stark contrast to the earlier discussion that required a 2D spatial structure for the field to be non-diffracting. The spatial structure likewise affects what is possible in the temporal domain. Surprisingly, there is a limit to how much OAM can be packed into a desired time pulse, with the OAM limiting the temporal width to $\Delta t \geq \sqrt{|\ell|}/\bar{\omega}$ along the bright caustic, while the central frequency, $\bar{\omega}$ is blueshifted as one approaches the spatial vortex[82]. Thus, space–time coupling not only manifests during propagation but also sets fundamental limits on what is possible with structured light.

Towards a nonlinear toolkit

Structured light through nonlinear crystals has been studied from the perspective of OAM for over 20 years. More recently, studies have revealed the influence of the light's phase, polarization and amplitude on the processes. For example, the excitation of radial (p) modes from $p = 0$ pump light has been explained as 'diffraction' from the amplitude structure of the pump[83]. The role of spin–orbit interactions in nonlinear processes when excited by vectorially structured light is still in its infancy, yet demonstrating impressive control over the excited structured light field[84]. These principles have been applied for the creation and detection of arbitrary structured light fields by upconversion[85], as well as for conversion of one structured light mode to another[86], illustrated in Fig. 2. The interplay of both linear and nonlinear processes with structured light likewise holds tremendous promise for extending the existing creation and detection toolkit[87].

Beyond crystals, nonlinear wave mixing in atomic vapour is rapidly leading to advances in the transfer, storage and detection toolkits[88], not only with OAM but also to imprint arbitrary structures into atomic vapour from the pump[89] including both fast and cheap approaches using digital micromirror devices[90]. OAM remains topical as a new parameter to control in structuring light through high-harmonic generation, where ultrafast laser pulses are coherently upconverted into the extreme ultraviolet and X-ray regions of the spectrum. These include attosecond high-harmonic beams with spatially controlled spin and orbital angular momentum states[91,92] and a time-varying OAM[93]. Here the notion of interference returns, but through a superposition of two time (delayed) pulses, each carrying a different OAM. Just as two or more OAM modes with different wavevectors results in a rotation and even acceleration during propagation in space, so the interference of two (or more) time-varying OAM pulses gives rise to a 'self-torque'. Spatiotemporal optical vortices are created spontaneously during nonlinear light–matter interactions, for example, optical pulse collapse and filamentation in air[94], analogous to the creation of spatial optical vortices in random media, for example, the atmosphere.

Finally, there are forms of structured light predicted where a nonlinear toolkit is crucial. One example is the 'flying doughnut', illustrated in Fig. 1g. This is a single-cycle toroidal pulse with a doughnut-like configuration of electric and magnetic fields[95], one of the many exotic 4D pulses that are allowed by Maxwell's equations that remain mostly unrealized in the laboratory[96], but may be edging closer to realization through nonlinear metasurfaces[97].

Pushing the limits

The potential of many millions of modes in a tiny cross-section area of light has the capacity to transform our communications networks in speed, while their quantum counterparts promise enhanced security by harnessing structured light as high-dimensional quantum states. Yet we seem restricted in how far the limits can be pushed.

Farther and faster. A main driver for progress in structured light over the past decade has been optical communications, where more modes means 'faster' communication (see ref. [98] and references therein). In a seminal demonstration, and still the state of the art, structuring the light so that each of 26 modes is a channel has enabled petabits-per-second data rates in the laboratory[99], but with a far slower speed and reach in free space of 80 gigabits per second over 260 metres[100]. The challenges are primarily turbulence and divergence, so that long-distance demonstrations have been limited to propagating without data transfer[101,102]. Developments in custom optical fibre for structured light is starting to show promise, reaching 50 km with eight modes[103], but still requiring error correction,
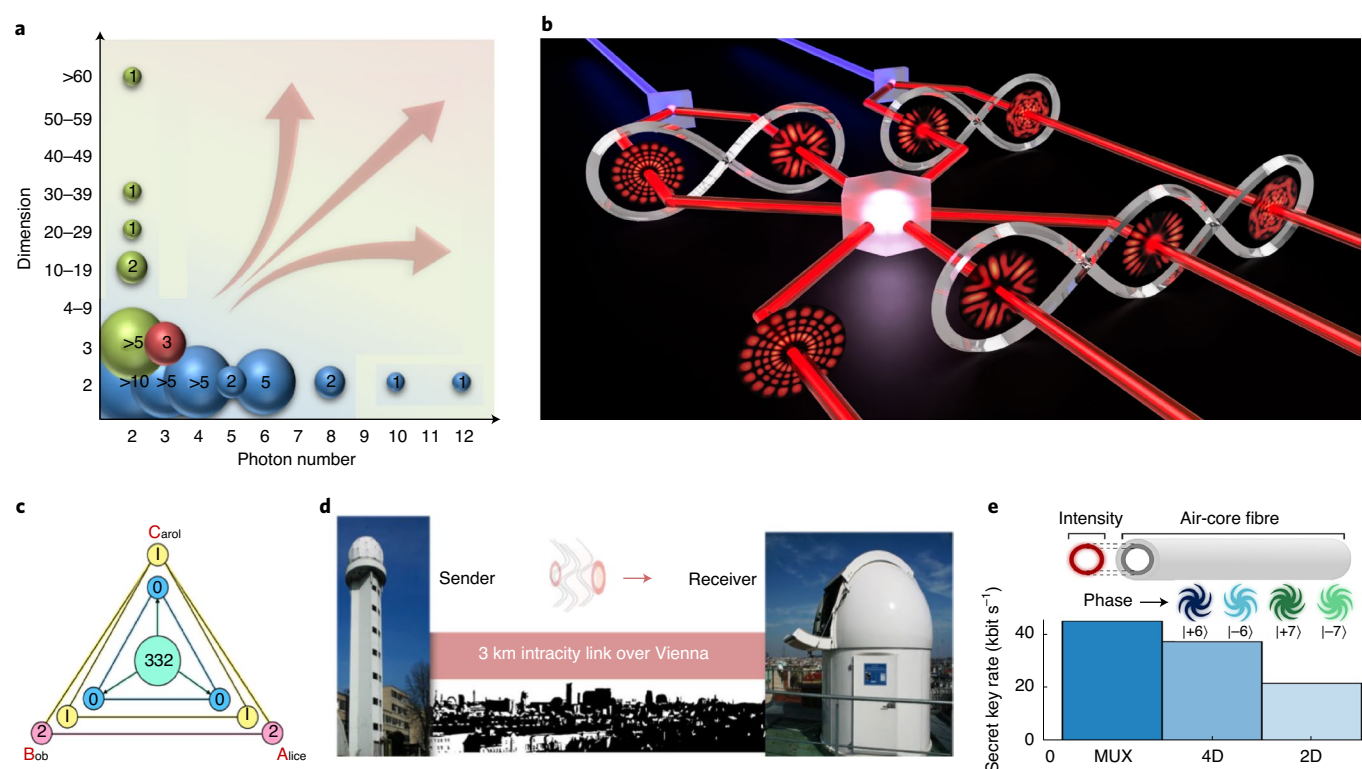
Fig. 3 | Pushing the limits of structured light. a, Recent developments have focused on advancing either the photon number (blue) or state dimension (green) of entangled photons, with progress in advancing them in concert (red) being hindered by an incomplete toolkit. Numbers in the bubbles indicate published studies in the field. **b**, In this artistic impression of multipartite entanglement by harnessing the natural high dimensionality of downconverted photon pairs, the cornerstone of generating such entangled states is a multiport device that enables the coherent manipulation of several photons in high dimensions. Such a device has yet to be realized. **c**, Recently, extending both the photon number and dimension beyond two has enabled layered quantum communication tasks, in which information is asymmetrically shared between participants. **d,e**, The adoption of structured photons in quantum networks rests in their distribution over long distances, which has seen recent advances in free space reaching 3 km (**d**) and high-dimensional QKD in the kilometre regime in optical fibre, with results showing that multiplexing 2D states (MUX) might, in the end, be a more attractive choice over high-dimensional QKD (**e**). Panels adapted with permission from: **c**, ref. [112], Springer Nature Ltd; **d**, ref. [121], PNAS; **e**, ref. [125], APS.

modest distances when compared with using Gaussian beams in single-mode fibre. While mode division multiplexing offers the potential for higher bit rates using complete families of structured light[104], the other side of the coin is diversity, holding the potential for lowering the error rates due to noise. It requires that the families of structured light behave differently in a particular medium, say turbulence or optical fibre, a fact not yet established. If diversity could be successfully implemented to counter noise, then the reach would be farther, perhaps even doubling in some cases[105].

Loss is equally problematic: in free space, light intensity has a roughly quadratic loss with distance, much better than the exponential loss in optical fibre. To address this requires amplification of structured light, particularly inside custom optical fibre, a new topic of exploration and initially limited to low order modes[106]. Since this seminal work, advances have pushed up the number of modes to 18 across modest wavelength bands in fibre[107], still far from what is required. Without amplification stages, the modern single-mode fibre network would not function at all, and this is certainly true for the proposed multimodal structured light network of the future.

Higher dimensions and more photons. Since the seminal work with spatial mode entanglement 20 years ago[108], the vast majority of studies have remained in the 2D realm both in photon number and state dimension, shown graphically in Fig. 3a. Yet the promise of higher information capacity, robustness to noise and better security require high-dimensional states, while more photons are needed to

realize quantum protocols such as teleportation and entanglement swapping, the cornerstone of a modern quantum network. The hurdles to overcome include very inefficient generation methods, and virtually no tools at all for the manipulation and deterministic detection of structured quantum states (a missing core tool is shown artistically in Fig. 3b), in stark contrast to their polarization qubit counterparts.

Recent efforts to address this, extending the two-photon qubit 'boundary' (Fig. 3a), have reached milestones in two directions: increasing the dimensionality of entangled photon pairs up to 100×100 dimensions[109], and increasing the number of qubits, reaching 12-photon polarization entanglement at a costly 1 count per hour coincidence rate[110]. The coupling of three DoFs (that is, path, polarization and OAM) with 6 photons has allowed for 18-qubit control[111] with an $\sim 10^{13}$ efficiency enhancement than if only a single DoF was used, demonstrating the advantage of hybrid entangled states. Mixing dimensions has also proved beneficial, such as the entangling of three photons, of which two were entangled in three dimensions, while the third was encoded as a qubit[112]. This arrangement allows for the entanglement, and in turn information, to be asymmetrically shared, enabling innovative layered quantum communication protocols, shown in Fig. 3c. An exciting development has been the use of machine learning and artificial intelligence to design quantum experiments in high dimensions: MELVIN[113] was used to find an appropriate experimental setup to realize a 3D triphoton state[114]. These ongoing efforts, combined with recent

developments including teleportation and entanglement swapped spatial photons[115], qutrit teleportation[116] and high-dimensional quantum memories for structured light[117], will speed up progress towards a global quantum network enabled by structured photons.

Fast and secure. The benefit of increased information capacity, security and noise resistance has become an important pacesetter for driving quantum key distribution (QKD) using high-dimensional structured photons, with early protocols shown up to $d = 8$ dimensions with entangled and single-photon OAM states, later extended to other mode types and protocols. The spatial mode basis not only offers more dimensions but also benefits from the properties of the basis itself (see ref. [118] and references therein). For example, Bessel entangled states are self-healing and non-diffracting, and have been exploited for QKD and entanglement transport through obstacles. Recent drives have been towards using all DoFs, through polarization, radial mode and OAM encoding[119], more than doubling the secure key rate possible with just polarization.

While we have seen profound developments in the generation and manipulation of structured quantum states, their reliable transmission remains a challenge, frustrated by similar obstacles to classical communication but without the ability to easily probe and correct. Both empirical data and rigorous theory suggest that the maximum reach before qubit OAM entanglement decays is $L_{max} \propto |\ell|^{5/6}$ in free space where ℓ is the initial OAM subspace[120]. Low-dimensional OAM states travel on the order of ~10 km before decaying (under moderate conditions), consistent with real-world demonstrations in free space of up to 3 km with 2D OAM entangled states[121], shown in Fig. 3d, and four high-dimensional single-photon hybrid states over a 300 m intracity free-space link[122], hindered by turbulence[123]. Fibre links do not fare much better, often requiring custom fibre to prevent state decoherence and intermodal dispersion. Three-dimensional[124] and four-dimensional[125] quantum transport has been demonstrated in the kilometre regime using custom fibre (Fig. 3e), the latter hinting that perhaps multiple 2D QKD is more effective than high-dimensional QKD, a notion recently employed to demonstrate multidimensional QKD over 250 m of single-mode fibre with hybrid entangled states[126], offering an alternative approach to the transmission of high-dimensional spatial modes over custom fibre. Notwithstanding the fact that there are still many milestones to be reached before we see any real-world deployments, a global quantum network remains conceivable.

Outlook

Despite a history spanning more than 200 years, structuring light has enjoyed a resurgence of late. Advances have spanned classical to quantum light, and fundamental science to real-world applications. In reviewing the progress, we have at times hinted at the open challenges. These include an incomplete toolkit for the creation, manipulation and detection of structured quantum states, the need for structured light demonstrations at higher powers for industrial applications, and transfer from bulk optics to compact on-chip technology for integrated solutions, particularly for optical communications. In parallel to the technological advances is our deeper understanding of the possibilities that structured light brings, and this is sure to fuel rapid advances in the future.

References

1. Karny, Z., Lavi, S. & Kafri, O. Direct determination of the number of transverse modes of a light beam. *Opt. Lett.* **8**, 409–411 (1983).
2. Lazarev, G., Chen, P.-J., Strauss, J., Fontaine, N. & Forbes, A. Beyond the display: phase-only liquid crystal on silicon devices and their applications in photonics. *Opt. Express* **27**, 16206–16249 (2019).
3. Ren, Y.-X., Lu, R.-D. & Gong, L. Tailoring light with a digital micromirror device. *Ann. Phys.* **527**, 447–470 (2015).
4. Turtaev, S. et al. Comparison of nematic liquid-crystal and DMD based spatial light modulation in complex photonics. *Opt. Express* **25**, 29874–29884 (2017).
5. Rubano, A., Cardano, F., Piccirillo, B. & Marrucci, L. Q-plate technology: a progress review. *J. Opt. Soc. Am. B* **36**, D70–D87 (2019).
6. Cardano, F. & Marrucci, L. Spin-orbit photonics. *Nat. Photon.* **9**, 776–778 (2015).
7. Bliokh, K. Y., Rodríguez-Fortuno, F., Nori, F. & Zayats, A. V. Spin–orbit interactions of light. *Nat. Photon.* **9**, 796–808 (2015).
8. Marrucci, L. et al. Spin-to-orbital conversion of the angular momentum of light and its classical and quantum applications. *J. Opt.* **13**, 064001 (2011).
9. Forbes, A. Structured light from lasers. *Laser Photon. Rev.* **13**, 1900140 (2019).
10. Padgett, M. J. Orbital angular momentum 25 years on. *Opt. Express* **25**, 11265–11274 (2017).
11. Shen, Y. et al. Optical vortices 30 years on: OAM manipulation from topological charge to multiple singularities. *Light Sci. Appl.* **8**, 90 (2019).
12. Young, T. I. The Bakerian Lecture. Experiments and calculations relative to physical optics. *Phil. Trans. R. Soc. A* **94**, 1–16 (1804).
13. Rubinsztein-Dunlop, H. et al. Roadmap on structured light. *J. Opt.* **19**, 013001 (2017).
14. Andrews, D. L. *Structured Light and its Applications: An Introduction to Phase-structured Beams and Nanoscale Optical Forces* (Academic Press, 2011).
15. Kogelnik, H. & Li, T. Laser beams and resonators. *Appl. Opt.* **5**, 1550–1567 (1966).
16. He, H., Friese, M., Heckenberg, N. & Rubinsztein-Dunlop, H. Direct observation of transfer of angular momentum to absorptive particles from a laser beam with a phase singularity. *Phys. Rev. Lett.* **75**, 826–829 (1995).
17. Heckenberg, N., McDuff, R., Smith, C. & White, A. Generation of optical phase singularities by computer-generated holograms. *Opt. Lett.* **17**, 221–223 (1992).
18. Padgett, M. J. & Courtial, J. Poincare-sphere equivalent for light beams containing orbital angular momentum. *Opt. Lett.* **24**, 430–432 (1999).
19. Holleczek, A., Aiello, A., Gabriel, C., Marquardt, C. & Leuchs, G. Classical and quantum properties of cylindrically polarized states of light. *Opt. Express* **19**, 9714–9736 (2011).
20. Milione, G., Sztul, H. I., Nolan, D. A. & Alfano, R. R. Higher-order poincare sphere, Stokes parameters, and the angular momentum of light. *Phys. Rev. Lett.* **107**, 053601 (2011).
21. Alonso, M. A. & Dennis, M. R. Ray-optical Poincare sphere for structured Gaussian beams. *Optica* **4**, 476–486 (2017).
22. Gutierrez-Cuevas, R., Dennis, M. & Alonso, M. Generalized Gaussian beams in terms of Jones vectors. *J. Opt.* **21**, 084001 (2019).
23. Nye, J. *Natural Focusing and Fine Structure of Light: Caustics and Wave Dislocations* (Institute of Physics, 1999).
24. Dennis, M., O'Holleran, K. & Padgett, M. Orbital angular momentum of light and the transformation of Laguerre–Gaussian laser modes. *Prog. Opt.* **53**, 293–363 (2009).
25. Stratton, J. *Electromagnetic Theory* (John Wiley and Sons, 1941).
26. Mazilu, M., Stevenson, D. J., Gunn-Moore, F. & Dholakia, K. Light beats the spread: "nondiffracting" beams. *Laser Photon. Rev.* **4**, 529–547 (2010).
27. Gutiérrez-Vega, J. C., Iturbe-Castillo, M. D. & Chávez-Cerda, S. Alternative formulation for invariant optical fields: Mathieu beams. *Opt. Lett.* **25**, 1493–1495 (2000).
28. Bandres, M. A. & Gutiérrez-Vega, J. C. Ince–Gaussian beams. *Opt. Lett.* **29**, 144–146 (2004).
29. Bandres, M. A., Gutiérrez-Vega, J. C. & Chávez-Cerda, S. Parabolic nondiffracting optical wave fields. *Opt. Lett.* **29**, 44–46 (2004).
30. Gutiérrez-Vega, J. C. & Bandres, M. A. Helmholtz–Gauss waves. *J. Opt. Soc. Am. A* **22**, 289–298 (2005).
31. Stoler, D. Operator methods in physical optics. *J. Opt. Soc. Am.* **71**, 334–341 (1981).
32. Dennis, M. R. & Alonso, M. A. Gaussian mode families from systems of rays. *J. Phys. Photon.* **1**, 025003 (2019).
33. Efremidis, N. K., Chen, Z., Segev, M. & Christodoulides, D. N. Airy beams and accelerating waves: an overview of recent advances. *Optica* **6**, 686–701 (2019).
34. Berry, M. V. & Balazs, N. L. Non-spreading wave packets. *Am. J. Phys.* **47**, 264–267 (1979).
35. Spreeuw, R. J. A classical analogy of entanglement. *Found. Phys.* **28**, 361–374 (1998).
36. Soukoulis, C. M. & Wegener, M. Past achievements and future challenges in the development of three-dimensional photonic metamaterials. *Nat. Photon.* **5**, 523–530 (2011).
37. Slussarenko, S. et al. Guiding light via geometric phases. *Nat. Photon.* **10**, 571–575 (2016).

38. He, C. et al. Complex vectorial optics through gradient index lens cascades. *Nat. Commun.* **10**, 4264 (2019).

39. D'Errico, A. et al. Two-dimensional topological quantum walks in the momentum space of structured light. *Optica* **7**, 108–114 (2020).

40. Cardano, F. et al. Quantum walks and wavepacket dynamics on a lattice with twisted photons. *Sci. Adv.* **1**, e1500087 (2015).

41. Fontaine, N. K. et al. Laguerre-Gaussian mode sorter. *Nat. Commun.* **10**, 1865 (2019).

42. Brandt, F., Hiekkämäki, M., Bouchard, F., Huber, M. & Fickler, R. High-dimensional quantum gates using full-field spatial modes of photons. *Optica* **7**, 98–107 (2020).

43. Berry, M. & Klein, S. Integer, fractional and fractal Talbot effects. *J. Mod. Opt.* **43**, 2139–2164 (1996).

44. Lopez-Mariscal, C. & Helmerson, K. Shaped nondiffracting beams. *Opt. Lett.* **35**, 1215–1217 (2010).

45. Hu, Y. et al. Subwavelength generation of nondiffracting structured light beams. *Optica* **7**, 1261–1266 (2020).

46. Huisken, J., Swoger, J., Del Bene, F., Wittbrodt, J. & Stelzer, E. H. Optical sectioning deep inside live embryos by selective plane illumination microscopy. *Science* **305**, 1007–1009 (2004).

47. Fahrbach, F. O., Simon, P. & Rohrbach, A. Microscopy with self-reconstructing beams. *Nat. Photon.* **4**, 780–785 (2010).

48. Vettenburg, T. et al. Light-sheet microscopy using an airy beam. *Nat. Methods* **11**, 541–544 (2014).

49. Zamboni-Rached, M. Stationary optical wave fields with arbitrary longitudinal shape by superposing equal frequency bessel beams: frozen waves. *Opt. Express* **12**, 4001–4006 (2004).

50. Dorrah, A. H., Zamboni-Rached, M. & Mojahedi, M. Wavelength and topological charge management along the axis of propagation of multichromatic non-diffracting beams. *J. Opt. Soc. Am. B* **36**, 1867–1872 (2019).

51. Aborahama, Y., Dorrah, A. H. & Mojahedi, M. Designing the phase and amplitude of scalar optical fields in three dimensions. *Opt. Express* **28**, 24721–24730 (2020).

52. Nylk, J. et al. Light-sheet microscopy with attenuation-compensated propagation-invariant beams. *Sci. Adv.* **4**, eaar4817 (2018).

53. Perez-Leija, A. et al. Discrete-like diffraction dynamics in free space. *Opt. Express* **21**, 17951–17960 (2013).

54. Eichelkraut, T. et al. Coherent random walks in free space. *Optica* **1**, 268–271 (2014).

55. Schulze, C. et al. Accelerated rotation with orbital angular momentum modes. *Phys. Rev. A* **91**, 043821 (2015).

56. Vetter, C., Eichelkraut, T., Ornigotti, M. & Szameit, A. Generalized radially self-accelerating helicon beams. *Phys. Rev. Lett.* **113**, 183901 (2014).

57. Efremidis, N. K. & Christodoulides, D. N. Abruptly autofocusing waves. *Opt. Lett.* **35**, 4045–4047 (2010).

58. Ayuso, D. et al. Synthetic chiral light for efficient control of chiral light–matter interaction. *Nat. Photon.* **13**, 866–871 (2019).

59. Maucher, F., Skupin, S., Gardiner, S. & Hughes, I. Creating complex optical longitudinal polarization structures. *Phys. Rev. Lett.* **120**, 163903 (2018).

60. Maucher, F., Skupin, S., Gardiner, S. & Hughes, I. An intuitive approach to structuring the three electric field components of light. *New J. Phys.* **21**, 013032 (2019).

61. Otte, E., Alpmann, C. & Denz, C. Polarization singularity explosions in tailored light fields. *Laser Photon. Rev.* **12**, 1700200 (2018).

62. Otte, E., Rosales-Guzman, C., Ndagano, B., Denz, C. & Forbes, A. Entanglement beating in free space through spin–orbit coupling. *Light Sci. Appl.* **7**, 18009 (2018).

63. Van Kruining, K., Cameron, R. & Gotte, J. Superpositions of up to six plane waves without electric-field interference. *Optica* **5**, 1091–1098 (2018).

64. Baüer, T. et al. Observation of optical polarization Möbius strips. *Science* **347**, 964–966 (2015).

65. Larocque, H. et al. Reconstructing the topology of optical polarization knots. *Nat. Phys.* **14**, 1079–1082 (2018).

66. Aiello, A., Banzer, P., Neugebauer, M. & Leuchs, G. From transverse angular momentum to photonic wheels. *Nat. Photon.* **9**, 789–795 (2015).

67. Bekshaev, A. Y., Bliokh, K. Y. & Nori, F. Transverse spin and momentum in two-wave interference. *Phys. Rev. X* **5**, 011039 (2015).

68. Eismann, J. et al. Transverse spinning of unpolarized light. *Nat. Photon.* **15**, 156–161 (2021).

69. Lindfors, K. et al. Local polarization of tightly focused unpolarized light. *Nat. Photon.* **1**, 228–231 (2007).

70. Weiner, A. M. Ultrafast optical pulse shaping: a tutorial review. *Opt. Commun.* **284**, 3669–3692 (2011).

71. Nassiri, M. G. & Brasselet, E. Multispectral management of the photon orbital angular momentum. *Phys. Rev. Lett.* **121**, 213901 (2018).

72. Shaltout, A. M., Shalaev, V. M. & Brongersma, M. L. Spatiotemporal light control with active metasurfaces. *Science* **364**, eaat3100 (2019).

73. Shaltout, A. M. et al. Spatiotemporal light control with frequency-gradient metasurfaces. *Science* **365**, 374–377 (2019).

74. Dallaire, M., McCarthy, N. & Piché, M. Spatiotemporal Bessel beams: theory and experiments. *Opt. Express* **17**, 18148–18164 (2009).

75. Chong, A., Wan, C., Chen, J. & Zhan, Q. Generation of spatiotemporal optical vortices with controllable transverse orbital angular momentum. *Nat. Photon.* **14**, 350–354 (2020).

76. Frei, F., Galler, A. & Feurer, T. Space–time coupling in femtosecond pulse shaping and its effects on coherent control. *J. Chem. Phys.* **130**, 034302 (2009).

77. Pariente, G., Gallet, V., Borot, A., Gobert, O. & Quéré, F. Space–time characterization of ultra-intense femtosecond laser beams. *Nat. Photon.* **10**, 547–553 (2016).

78. Sun, B. et al. Four-dimensional light shaping: manipulating ultrafast spatiotemporal foci in space and time. *Light Sci. Appl.* **7**, 17117 (2018).

79. Mosk, A. P., Lagendijk, A., Lerosey, G. & Fink, M. Controlling waves in space and time for imaging and focusing in complex media. *Nat. Photon.* **6**, 283–292 (2012).

80. Kondakci, H. E. & Abouraddy, A. F. Diffraction-free pulsed optical beams via space–time correlations. *Opt. Express* **24**, 28659–28668 (2016).

81. Kondakci, H. E. & Abouraddy, A. F. Diffraction-free space–time light sheets. *Nat. Photon.* **11**, 733–740 (2017).

82. Porras, M. A. & Conti, C. Couplings between the temporal and orbital angular momentum degrees of freedom in ultrafast optical vortices. *Phys. Rev. A* **101**, 063803 (2020).

83. Buono, W. et al. Chiral relations and radial-angular coupling in nonlinear interactions of optical vortices. *Phys. Rev. A* **101**, 043821 (2020).

84. Wu, H.-J. et al. Vectorial nonlinear optics: type-II second-harmonic generation driven by spin–orbit-coupled fields. *Phys. Rev. A* **100**, 053840 (2019).

85. Sephton, B. et al. Spatial mode detection by frequency upconversion. *Opt. Lett.* **44**, 586–589 (2019).

86. Pires, D., Rocha, J., Jesus-Silva, A. & Fonseca, E. Optical mode conversion through nonlinear two-wave mixing. *Phys. Rev. A* **100**, 043819 (2019).

87. Tang, Y. et al. Harmonic spin–orbit angular momentum cascade in nonlinear optical crystals. *Nat. Photon.* **14**, 658–662 (2020).

88. Franke-Arnold, S. Optical angular momentum and atoms. *Phil. Trans. R. Soc. A* **375**, 20150435 (2017).

89. Boyer, V., Marino, A. M., Pooser, R. C. & Lett, P. D. Entangled images from four-wave mixing. *Science* **321**, 544–547 (2008).

90. Gauthier, G. et al. Direct imaging of a digital-micromirror device for configurable microscopic optical potentials. *Optica* **3**, 1136–1143 (2016).

91. Kong, F. et al. Controlling the orbital angular momentum of high harmonic vortices. *Nat. Commun.* **8**, 14970 (2017).

92. Dorney, K. M. et al. Controlling the polarization and vortex charge of attosecond high-harmonic beams via simultaneous spin–orbit momentum conservation. *Nat. Photon.* **13**, 123–130 (2019).

93. Rego, L. et al. Generation of extreme-ultraviolet beams with time-varying orbital angular momentum. *Science* **364**, eaaw9486 (2019).

94. Jhajj, N. et al. Spatiotemporal optical vortices. *Phys. Rev. X* **6**, 031037 (2016).

95. Hellwarth, R. & Nouchi, P. Focused one-cycle electromagnetic pulses. *Phys. Rev. E* **54**, 889–895 (1996).

96. Papasimakis, N., Fedotov, V., Savinov, V., Raybould, T. & Zheludev, N. Electromagnetic toroidal excitations in matter and free space. *Nat. Mater.* **15**, 263–271 (2016).

97. Keren-Zur, S., Tal, M., Fleischer, S., Mittleman, D. M. & Ellenbogen, T. Generation of spatiotemporally tailored terahertz wavepackets by nonlinear metasurfaces. *Nat. Commun.* **10**, 1778 (2019).

98. Trichili, A., Park, K.-H., Zghal, M., Ooi, B. S. & Alouini, M.-S. Communicating using spatial mode multiplexing: potentials, challenges, and perspectives. *IEEE Commun. Surv. Tutor.* **21**, 3175–3203 (2019).

99. Wang, J. et al. N-dimensional multiplexing link with 1.036-Pbit/s transmission capacity and 112.6-bit/s/Hz spectral efficiency using OFDM-8QAM signals over 368 WDM pol-muxed 26 OAM modes. In *2014 The European Conference on Optical Communication (ECOC)* 1–3 (IEEE, 2014).

100. Zhao, Y. et al. Experimental demonstration of 260-meter security free-space optical data transmission using 16-QAM carrying orbital angular momentum (OAM) beams multiplexing. In *Optical Fiber Communication Conference* Th1H–3 (Optical Society of America, 2016).

101. Lavery, M. P. et al. Free-space propagation of high-dimensional structured optical fields in an urban environment. *Sci. Adv.* **3**, e1700552 (2017).

102. Krenn, M. et al. Twisted light transmission over 143 km. *Proc. Natl Acad. Sci. USA* **113**, 13648–13653 (2016).

103. Wen, Y. et al. Compact and high-performance vortex mode sorter for multi-dimensional multiplexed fiber communication systems. *Optica* **7**, 254–262 (2020).

104. Zhao, N., Li, X., Li, G. & Kahn, J. M. Capacity limits of spatially multiplexed free-space communication. *Nat. Photon.* **9**, 822–826 (2015).

105. Cox, M. A., Cheng, L., Rosales-Guzmán, C. & Forbes, A. Modal diversity for robust free-space optical communications. *Phys. Rev. Appl.* **10**, 024020 (2018).

106. Jung, Y. et al. Optical orbital angular momentum amplifier based on an air-hole erbium-doped fiber. *J. Light. Tech.* **35**, 430–436 (2017).

107. Ma, J., Xia, F., Chen, S., Li, S. & Wang, J. Amplification of 18 OAM modes in a ring-core erbium-doped fiber with low differential modal gain. *Opt. Express* **27**, 38087–38097 (2019).

108. Mair, A., Vaziri, A., Weihs, G. & Zeilinger, A. Entanglement of the orbital angular momentum states of photons. *Nature* **412**, 313–316 (2001).

109. Krenn, M. et al. Generation and confirmation of a (100×100)-dimensional entangled quantum system. *Proc. Natl Acad. Sci. USA* **111**, 6243–6247 (2014).

110. Zhong, H.-S. et al. 12-photon entanglement and scalable scattershot boson sampling with optimal entangled-photon pairs from parametric down-conversion. *Phys. Rev. Lett.* **121**, 250505 (2018).

111. Wang, X.-L. et al. 18-qubit entanglement with six photons? Three degrees of freedom. *Phys. Rev. Lett.* **120**, 260502 (2018).

112. Malik, M. et al. Multi-photon entanglement in high dimensions. *Nat. Photon.* **10**, 248–252 (2016).

113. Krenn, M., Malik, M., Fickler, R., Lapkiewicz, R. & Zeilinger, A. Automated search for new quantum experiments. *Phys. Rev. Lett.* **116**, 090405 (2016).

114. Erhard, M., Malik, M., Krenn, M. & Zeilinger, A. Experimental Greenberger–Horne–Zeilinger entanglement beyond qubits. *Nat. Photon.* **12**, 759–764 (2018).

115. Zhang, Y. et al. Simultaneous entanglement swapping of multiple orbital angular momentum states of light. *Nat. Commun.* **8**, 632 (2017).

116. Luo, Y.-H. et al. Quantum teleportation in high dimensions. *Phys. Rev. Lett.* **123**, 070505 (2019).

117. Shi, B.-S., Ding, D.-S. & Zhang, W. Quantum storage of orbital angular momentum entanglement in cold atomic ensembles. *J. Phys. B* **51**, 032004 (2018).

118. Forbes, A. & Nape, I. Quantum mechanics with patterns of light: progress in high dimensional and multidimensional entanglement with structured light. *AVS Quantum Sci.* **1**, 011701 (2019).

119. Zhou, Y. et al. Using all transverse degrees of freedom in quantum communications based on a generic mode sorter. *Opt. Express* **27**, 10383–10394 (2019).

120. Leonhard, N. D., Shatokhin, V. N. & Buchleitner, A. Universal entanglement decay of photonic-orbital-angular-momentum qubit states in atmospheric turbulence. *Phys. Rev. A* **91**, 012345 (2015).

121. Krenn, M., Handsteiner, J., Fink, M., Fickler, R. & Zeilinger, A. Twisted photon entanglement through turbulent air across Vienna. *Proc. Natl Acad. Sci. USA* **112**, 14197–14201 (2015).

122. Sit, A. et al. High-dimensional intracity quantum cryptography with structured photons. *Optica* **4**, 1006–1010 (2017).

123. Cox, M. A. et al. Structured light in turbulence. *IEEE J. Sel. Top. Quantum Electron.* **27**, 7500521 (2020).

124. Cao, H. et al. Distribution of high-dimensional orbital angular momentum entanglement over a 1 km few-mode fiber. *Optica* **7**, 232–237 (2020).

125. Cozzolino, D. et al. Orbital angular momentum states enabling fiber-based high-dimensional quantum communication. *Phys. Rev. Appl.* **11**, 064058 (2019).

126. Liu, J. et al. Multidimensional entanglement transport through single-mode fiber. *Sci. Adv.* **6**, 0837 (2020).

127. Abramochkin, E. & Volostnikov, V. Generalized Gaussian beams. *J. Opt. A* **6**, S157–S161 (2004).

128. Danakas, S. & Aravind, P. K. Analogies between two optical systems (photon beam splitters and laser beams) and two quantum systems (the two-dimensional oscillator and the two-dimensional hydrogen atom). *Phys. Rev. A* **45**, 1973–1977 (1992).